Synthesis of Side-Chain Liquid Crystalline Homopolymers and Block Copolymers with Well-Defined Structures by Living Anionic Polymerization and Their Thermotropic Phase Behavior

Masayuki Yamada, Tsukasa Iguchi, Akira Hirao, Seiichi Nakahama, and Junji Watanabe*

Department of Polymer Chemistry, Tokyo Institute of Technology, Ookayama, Meguro-ku, Tokyo 152, Japan

Received June 8, 1994; Revised Manuscript Received October 3, 1994®

ABSTRACT: This paper describes the synthesis of side-chain liquid crystalline polymers and block copolymers by living anionic polymerization and their thermotropic phase behavior. The polymers were successfully prepared with a narrow distribution of molecular weight. The thermotropic transition behavior between crystal, smectic A, and isotropic phases was examined with a function of the molecular weight. Living anionic polymerization also allowed the preparation of well-defined block copolymers with amorphous polystyrene. In these block copolymers, microphase separation due to liquid crystalline and amorphous blocks was observed by electron microscopy and small-angle X-ray methods. Effects of the microphase separation were also examined on the thermotropic phase behavior and structure.

Introduction

Polymer liquid crystals containing mesogenic groups in the side chains have been extensively studied in recent years.[1,2] Research interests have focused mainly on the influence of the nature and structure of mesogenic side-chain groups on the mesomorphic properties of the polymers. Another field of interest deals with the role of the main-chain backbone on the liquid crystal properties mainly by treating the polysiloxanes, polyacrylates, and polymethacrylates. The various parameters with respect to the main-chain backbone such as the degree of polymerization, molecular weight distribution, and monomer unit distribution in random and block copolymers can be considered.

An important breakthrough in the latter field has been performed by controlled polymerization, group-transfer polymerization and living polymerization, since these permit the control of several parameters given above because of the synthesis of well-defined structures.[3-8] Investigations of the well-defined polymers have established the precise relationship between structural parameters and thermotropic phase behavior.

In the first part of this study, we will report the synthesis of poly[6-[4-(4-methoxyphenyl)phenoxy]hexyl methacrylate] (termed here poly(**1**)) by living anionic

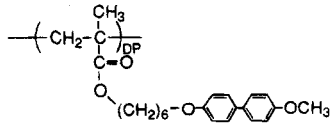

Poly(**1**)

polymerization. This polymer was first synthesized by Finkelmann et al.,[9] and its thermotropic liquid crystalline behavior has been examined with relation to the tacticity of the main-chain backbone. Further studies have been performed by preparing the highly isotactic (mm 90−97%) and syndiotactic (rr 79−86%) polymers.[10,11] The studies indicate that the tacticity is a significant factor on the formation of a thermotropic liquid crystal and in this limited polymeric system the liquid crystal was found to be preferentially formed from the syndiotactic polymer. The polymers prepared in this study are highly syndiotactic (rr 80%) with a relatively narrow distribution of molecular weight and with a molecular weight ranging from 3000 to 30 000. By using these well-defined polymers, we will examine the effect of molecular weight on the thermotropic phase behavior.

One of the most attractive features of living polymerization is the feasibility of synthesizing block copolymers with well-defined structures. In the second part of this study, we have also prepared a variety of monodisperse diblock copolymers composed of poly(**1**) and amorphous polystyrene blocks by living anionic polymerization. In this copolymer system, microphase separation with the liquid crystalline microphases will be expected and so the properties of two polymer classes will be closely bound to each other.[12-15] Here, the following combined effects can be considered.

1. The size and type of microphase separation, which can be controlled by the molecular weight and composition, may affect the phase transition of the liquid crystalline poly(**1**) block.
2. The connection of two polymer chains at the interface may affect the orientational and positional orders of the liquid crystaline phase because of a tendency that the main-chain backbone preferentially orients perpendicular to the interface.

Keeping these points in mind, the thermotropic phase behavior and structures of the block copolymers will be examined and compared with those exhibited by the homopolymers.

Experimental Section

Methods. Differential scanning calorimetric (DSC) measurements were carried out with a Perkin-Elmer DSC Model II at a scanning rate of 2 °C/min.

X-ray measurements were carried out by using a Rigaku-Denki X-ray generator with Ni-filtered Cu Kα radiation. The temperatures of the sample were regulated within 1 °C by using a Mettler FP-82 hot stage. Reflection spacings were calibrated by using a silicon standard.

The optical textures of the mesophases were studied using a polarizing microscope (an Olympus BH-2) equipped with a Mettler FP-82 hot stage.

The TEM observation to clarify the morphology of the block copolymers was performed by a Hitachi H-500 transmission

® Abstract published in *Advance ACS Abstracts,* November 15, 1994.

0024-9297/95/2228-0050$09.00/0

electron microscope with 100 kV of accelerating voltage. For this observation, an ultrathin section of the polymer film was prepared as follows. The polymer film was dipped in a 1 wt % aqueous solution of ruthenium tetraoxide (RuO_4) as the fixing and staining reagent for 20 min. After being dried, the film was embedded in an epoxy resin and cut into ultrathin sections (700–1000 Å thick) by an ultramicrotome with a diamond knife. The sectioned specimens were further stained with the vapor of RuO_4 for 5 min before observation.

Materials. Monomer, 6-[4-(4-methoxyphenyl)phenoxy]-hexyl methacrylate (MPPHM), was synthesized according to

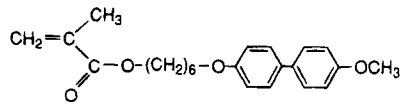

MPPHM

the previous paper.[10] It was dried over P_2O_5 for 48 h under a high vacuum condition (10^{-6} mmHg), diluted with dry THF to result in 0.05 M solutions, and placed in glass ampules. Styrene and 1,1-diphenylethylene were purified according to the standard method. Commercially available *sec*-butyllithium (s-BuLi) was diluted with heptane in glass ampules.

All the polymerizations of homopolymers were carried out at −78 to −40 °C with shaking under high vacuum conditions in all the glass apparatus equipped with break-seals. The details of the polymerization procedure are shown later. After an appropriate polymerization time, the polymerization mixture was poured into methanol to precipitate the polymer. It was purified by reprecipitation twice from THF to methanol. The molecular weight (M_n) and molecular weight distribution (M_w/M_n) were determined by a SEC profile based on the calibration of standard PMMA.

The block copolymers were obtained by a sequential addition of styrene and MPPHM under the similar reaction conditions. The composition of each segment was determined by ^1H NMR. The M_n and M_w/M_n values were estimated from a SEC profile based on the standard polystyrene calibration.

Results and Discussion

1. Anionic Polymerization of MPPHM Monomer. Although anionic polymerization of alkyl methacrylates have been extensively investigated so far, these monomers have ester functions susceptible to react with carbanionic species and therefore living polymerization systems are still limited in number even at the present time.

Teyssié and his co-workers[16,17] demonstrated in 1987 a striking additive effect of LiCl on the anionic polymerization of MMA and *tert*-butyl acrylate. PMMA prepared in the presence of LiCl had an extremely narrow distribution, with a M_w/M_n value as low as 1.02, and more importantly, the anionic polymerization of *tert*-butyl acrylate was found to become a living system for the first time by adding LiCl.[16] We have also recently found that 3-(trialkoxysilyl)propyl methacrylate[18] and (2,2-dimethyl-1,3-dioxolan-4-yl)methyl methacrylate[19] can undergo a living anionic polymerization by adding LiCl. The distributions of the molecular weight in the resultant polymers were narrow, with M_w/M_n ratios below 1.05. Considering these remarkable effects of LiCl on the anionic polymerizations of alkyl methacrylates, we have adopted here a similar polymerization reaction with LiCl with an attempt to control the polymerization and to result in polymers with a narrow distribution of molecular weight. The polymers obtained are listed with their characterization in Table 1, and their detailed synthetic routes are described below.

Initially, the polymerization of MPPHM monomer was carried out at −78 °C in THF with the initiator system including s-BuLi, 1,1-diphenylethylene, and LiCl (see Table 1). At this temperature, the polymerization system became cloudy immediately on addition of MPPHM and the polymer was precipitated as the polymerization proceeded. After 2 h, a quantitative yield of polymer was obtained. The molecular weight observed was found to correspond with that calculated from the ratio of [M]/[I]. However, the SEC analyses revealed the polymer to have a distribution with a hint of bimodality and a M_w/M_n of around 1.3. In this study, hence, the polymerization was performed at an elevated temperature of −40 °C with a hope to prevent the polymer precipitation during the polymerization. Under this condition, the polymerization system was homogeneous for the first few minutes but become heterogeneous with time. Interestingly, even such a small change in the polymerization event provided a beneficial effect on the molecular weight distribution of polymers. The resultant polymers usually have a unimodal distribution with M_w/M_n ratios as low as 1.1 when their molecular weights were less than 12 000 (see curve A in Figure 1 and Table 1). Good agreement between M_n values

Table 1. Anionic Polymerization of MPPHM in THF at −40 °C for 2 h[a]

sample	monomer MPPHM, mmol	initiator s-BuLi, mmol	DEP,[b] mmol	LiCl, mmol	$10^{-3}M_n$ calcd	$10^{-3}M_n$ obsd[c]	M_w/M_n[c]
poly(**1a**)	0.469	0.0613	0.119	0.277	3 200	3 300	1.09
poly(**1b**)	0.298	0.0273	0.048	0.095	4 200	4 700	1.13
poly(**1c**)	0.750	0.0436	0.152	0.167	6 500	7 000	1.05
poly(**1d**)	0.857	0.0465	0.136	0.220	6 900	7 800	1.07
poly(**1e**)[e]	0.876	0.0396	0.120	0.189	8 300	8 500	1.26
poly(**1f**)	0.758	0.0284	0.138	0.249	10 200	11 200	1.12
poly(**1g**)	1.17	0.0357	0.109	0.259	11 700	12 000	1.14
poly(**1h**)	0.718	0.0203	0.079	0.078	13 300	14 400	1.46
poly(**1i**)	1.31	0.0336	0.069	0.113	14 300	17 000	1.23
poly(**1j**)	1.15	0.0258	0.038	0.077	16 600	22 800	1.87
poly(**1k**)	0.942	0.0279	0.062	0.094	12 700	31 000	1.71

[a] Yields of polymers were quantitative. [b] 1,1-Diphenylethylene. [c] M_n(obsd) and M_w/M_n were determined by SEC using the calibration of standard PMMA. [d] M_w/M_n was determined by SEC. [e] This material was obtained by polymerization at −78 °C.

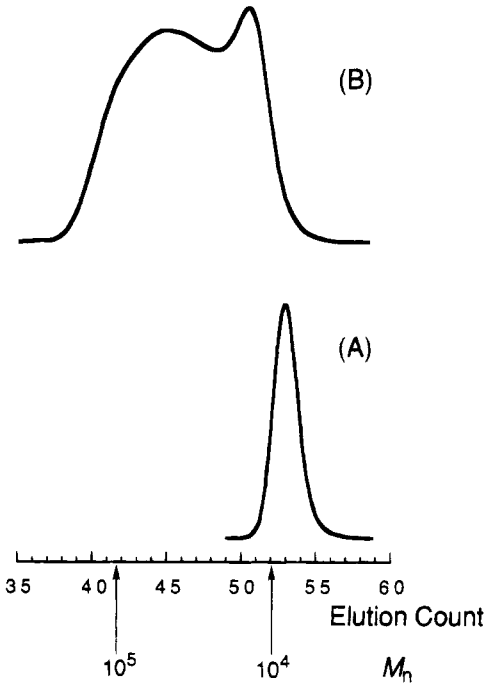

Figure 1. SEC charts of poly(**1**)s which were prepared by living anionic polymerization at −40 °C: (A) poly(**1c**) with M_n = 7000 and M_w/M_n = 1.05; (B) poly(**1j**) with M_n = 22 800 and M_w/M_n = 1.87.

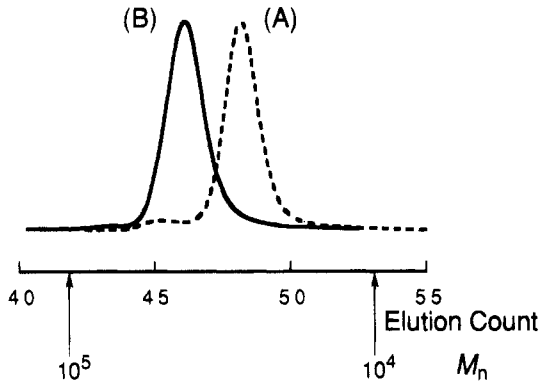

Figure 2. SEC charts of polystyrene and polystyrene-*block*-poly(**1**) which were prepared in the sequential polymerization: (A) polystyrene with M_n = 18 700 and M_w/M_n = 1.08; (B) poly(**2a**) with M_n = 33 700 and M_w/M_n = 1.03.

observed and calculated is also attained. These results indicate a living character of the polymerization of MPPHM at −40 °C.

At higher [M]/[I] ratios to achieve the higher molecular weight of more than 15 000, however, bimodal distributions were clearly observed in the SEC chart (curve B of Figure 1). In these cases, the observed M_n values were definitely higher than those calculated as found in Table 1. Accordingly, at the moment, the controlled polymerization of MPPHM can proceed to some extent, but it is interrupted by the significant polymer precipitation. As mentioned later, the transition temperatures of the poly(**1**)s prepared here level off at the M_n value of around 12 000. By this reason, further optimization of the polymerization condition has not been examined for this purpose. The proton NMR shows that the syndiotacticity of all the polymers obtained here is around 80%.

2. Block Copolymerization of Styrene with MPPHM. A variety of A−B block copolymers (termed here poly(**2**)) were prepared by the sequential polymerization

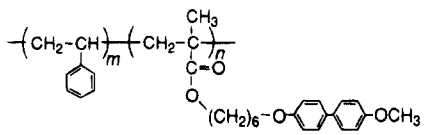

Poly(**2**)

of styrene as monomer A and MPPHM as monomer B. Living polystyrene was first prepared with s-BuLi in THF at −78 °C for 10 min. and then 1,1-diphenylethylene was added to cap the highly reactive polystyryl anion. The sequential polymerization of MPPHM was then carried out with this polymeric anion in the presence of LiCl in THF at −40 °C for 2 h. As can be seen in Figure 2, the block copolymer formed possessed a symmetrical unimodal peak with a narrow distribution, with a M_w/M_n value of 1.03. The polymerization was usually homogeneous but in some cases became heterogeneous because of the polymer precipitation. This is dependent on the molecular weight of the poly(**1**) block; the increase of the molecular weight of poly(**1**) tends to make the system heterogeneous. The polymers were obtained with the quantitative yields in all cases, possessing the predictable M_n values, compositions, and narrow molecular weight distributions. The results are summarized in Table 2. Here, the molecular weights of the block segments were varied in the range of 10 000−18 000, and the compositions of poly(**1**) segments ranged from 40 to 60 wt %. Interestingly, the molecular weight of the poly(**1**) segment could be

Table 2. Block Copolymerization of Styrene with MPPHM[a]

	polystyrene-*block*-poly(**1**)		
sample	M_n(calcd)	M_n(obsd)[b]	M_w/M_n[c]
poly(**2a**)	18 000−13 500	18 700−15 000	1.03
poly(**2b**)	14 000−11 440	15 000−15 000	1.04
poly(**2c**)	10 600−12 600	10 700−18 000	1.11

[a] Block copolymerization was carried out at −78 °C in THF by sequential addition of styrene with s-BuLi at first and then MPPHM after capping with 1,1-diphenylethylene and LiCl. Yields of polymers were quantitative in all runs. Polymerization times at the first and second stages were 0.2 and 4 h, respectively. [b] M_n(obsd) of the poly(MPPHM) segment was determined by ^{1}H NMR. [c] M_w/M_n was determined from a SEC profile based on the calibration of standard polystyrene.

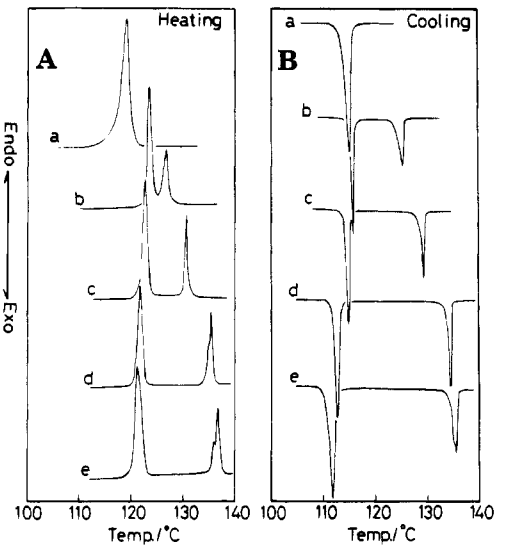

Figure 3. DSC thermograms of the poly(**1**)s: (A) second heating curves and (B) first cooling curves; (a) poly(**1a**), (b) poly(**1b**), (c) poly(**1d**), (d) poly(**1h**), and (e) poly(**1i**).

controlled, at least, up to 18 000 in the block copolymerization which is higher than that in the homopolymer system. This may result from an increase in the solubility of the polymer by virtue of incorporation of the polystyrene segment.

3. Thermotropic Phase Behavior and Structures of Poly(1). Thermal transitions of the poly(**1**)s were measured by DSC thermograms as shown in Figure 3. All DSC heating and cooling scans were identical when the same rates of 2 °C/min were applied, and the transitions included appear as sharp peaks. The transition temperatures and enthalpies are summarized in Table 3.

The transition temperatures due to heating and cooling scans are plotted as a function of the M_n in parts a and b of Figure 4. As found here, the polymers show two dominant transitions. One is a crystal melting to smectic A (S_A) at T_1 and another is a S_A−isotropic phase transition at T_2. The structural details of the crystal and smectic A will be described later by a combination of X-ray and optical microscopic observations. In all polymers, the crystallization takes place on cooling, and so no distinct glass transition appears.

Some exceptions exhibiting the dissimilarity can be observed. The lowest molecular weight oligomer (poly(**1a**)) with approximately 9 repeat units shows the direct transition of crystal to isotropic melt. In the higher molecular weight materials having a M_n of more than 12 000, on the other hand, another small transition along with the two transitions can be observed just

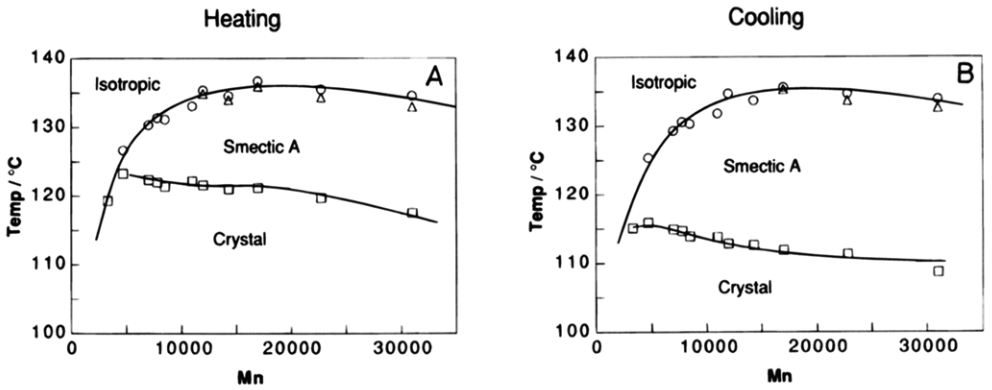

Figure 4. Dependence of the transition temperatures on the molecular weight of the poly(**1**)s based on (A) a second heating DSC scan and (B) a first cooling DSC scan.

Table 3. DSC Data of Poly(1)

	transition temp, °C (transition enthalpy, kcal/mol)			
	heating		cooling	
sample	T_1 (ΔH_1)	T_2 (ΔH_2)	T_1 (ΔH_1)	T_2 (ΔH_2)
poly(**1a**)	119.3 (2.39)		115.1 (2.35)	
poly(**1b**)	123.3 (1.49)	126.7 (0.65)	115.9 (1.43)	125.4 (0.82)
poly(**1c**)	122.4 (1.52)	130.4 (0.70)	114.9 (1.32)	129.3 (0.70)
poly(**1d**)	122.4 (1.45)	131.5 (0.76)	114.6 (1.24)	130.4 (0.66)
poly(**1e**)	121.4 (1.45)	131.2 (0.63)	113.9 (1.27)	130.3 (0.63)
poly(**1f**)	122.2 (1.36)	133.1 (0.60)	113.8 (1.14)	131.8 (0.60)
poly(**1g**)	121.6 (1.34)	134.9/135.4 (0.61)	112.8 (1.14)	134.7 (0.60)
poly(**1h**)	121.0 (1.41)	134.0/134.6 (0.63)	112.6 (1.21)	133.7 (0.62)
poly(**1i**)	121.2 (1.36)	135.9/136.7 (0.64)	111.9 (1.14)	135.3/136.3 (0.62)
poly(**1j**)	119.7 (1.37)	134.3/135.5 (0.58)	111.3 (1.18)	133.7/134.7 (0.58)
poly(**1k**)	117.5 (1.32)	133.0/134.6 (0.58)	108.7 (1.14)	132.6/133.9 (0.55)

below the isotropization temperature. This transition may be due to the smectic A to nematic phase transition, but the nematic phase is not definitely identified because of the extremely narrow temperature region.

X-ray diffraction studies were performed to clarify the phase structures. Figure 5 shows the X-ray pattern of the oriented fiber which was observed for the crystal of poly(**1j**). Here, the oriented fiber was prepared by pulling up an isotropic melt, and the fiber axis is placed in a vertical direction. In this crystal pattern, there are observed three inner reflections along the meridian and also several outer reflections with strong intensity along the equator. Although only the limited number of reflections are observed, the diffraction pattern is simple enough to allow a unique determination of the orthorhombic unit cell with parameters of $a = 8.04$ Å, $b = 5.45$ Å, and $c = 25.8$ Å[20] (refer to Table 4). The observed density of 1.17 g/mL dictates that two repeat units are included in this unit cell. Although the three-dimensional unit cell is given for convenience, the structure is understood to be of the layer type rather than of three-dimensional order since only the (hk0) and (00l) reflections can be observed. Within an individual layer, the side-chain biphenyl groups are crystallized into the two-dimensional lattice with $a = 8.04$ Å, $b = 5.45$ Å, and $\gamma = 90°$, which resembles that (with $a = 8.12$ Å, $b = 5.63$ Å, and $\gamma = 90°$) observed for the crystal of biphenyls.[21,22] These layers are piled up with a spacing of $c = 25.8$ Å.

In this layered crystalline phase, the more detailed structural aspects can be deduced from the two following facts. One is that the layer spacing of 25.8 Å corresponds roughly to the length of the side chain in a fully extended form. The fact is that the second layer reflection appears more intense than the first (see Figure 5), showing that there are two maximum peaks

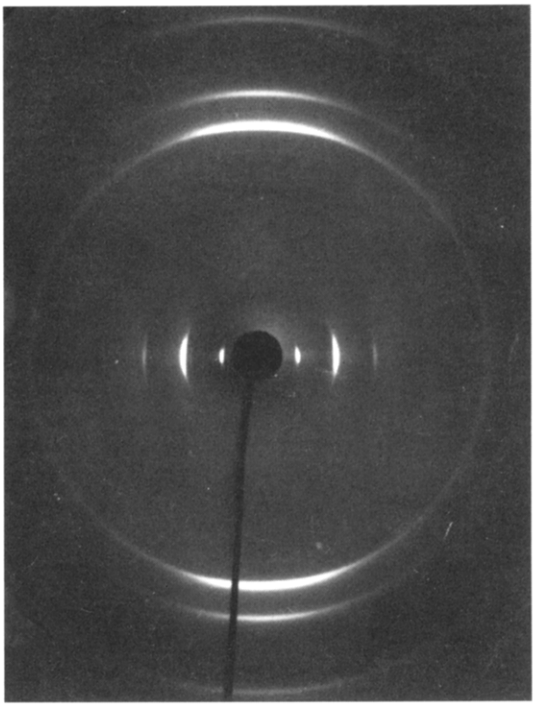

Figure 5. Oriented X-ray patterns of the crystalline phase as observed for the fibrous poly(**1j**). Here, the fiber specimen was prepared by drawing the isotropic melt, and its axis is placed in the vertical direction.

Table 4. X-ray Spacings (Å) of the Crystalline and Smectic A Phases in the Homopolymer and Block Copolymer[a]

poly(**1j**)		poly(**2a**)	
crystal	smectic A	crystal	smectic A
Small-Angle Region			
25.7 (001) m		25.8 (001) m	26.4 (001) vvw
12.9 (002) vs	13.2 (002) vw	12.8 (002) vs	13.2 (002) m
8.60 (003) w		8.58 (003) w	
Wide-Angle Region			
4.50 (110) s	~4.5 br	4.48 (110 s	~4.5 br
4.02 (200) m		3.99 (200) m	
3.24 (210) w		3.22 (210) w	
2.58 (120) vw		2.58 (120) vw	
2.39 (310) vw		2.38 (310) vw	
2.26 (220) vw			

[a] Indices are based on the unit cell cited in the text.

of electron density in a repeating length of 25.8 Å along the layer normal. According to these facts, we reach a plausible layered structure in which there is segregation into two regions composed of side-chain mesogens and main-chain backbones, and the mesogenic region is

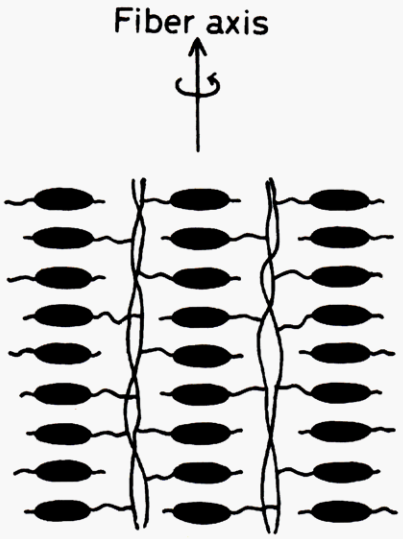

Figure 6. Schematic illustration of the plausible layered structure in the fibrous crystalline phase.

constructed by an assembly of randomly directed side-chain mesogens whose geometric axes coincide. The tentative layer structure is illustrated in Figure 6. Such a type of layered structure is often observed in this type of side-chain liquid crystalline polymer.[23-26]

On heating the sample to the smectic A temperatures, the outer reflections are altered to the broad hallow with a spacing of 4.5 Å. Simultaneously, the layer reflections on the meridian become appreciably weak, leaving only a very weak but detectable reflection with a spacing of 13.2 Å. The X-ray pattern, thus, is characteristic of the smectic A. Hahn et al.[10] have reported that no layer reflections can be detected, and so the ambiguity remained as to the assignment of the smectic A at least based on the X-ray analysis. The reason is not clear for this difference. The 13.2 Å of the layer reflection is too short as a layer thickness and may be half of the layer thickness. In fact, in the block copolymers which will be treated later, the 26.4-Å reflection can be observed as a first-order reflection although its intensity is remarkably weak in comparison with that of the second-order 13.2-Å reflection. We thus conclude that the smectic A has a layer thickness of 26.4 Å which is approximate to that in the layered crystal phase. The fairly weak appearance of layer reflections suggests the low layer order parameter of the smectic structure.

The crystal to S_A transition can also be detected from optical microscopy. Although the higher molecular weight specimen exhibits only an ambiguous change of the texture, the smectic A phase for the lower molecular weight specimen can be well identified from the characteristic fan-shaped texture. The typical texture is shown in Figure 7.

As a summary, all the polymers exhibiting two transitions show the same sequence of phases, crystal–S_A–isotropic phase sequence, and no significant effect of molecular weight can be observed on the phase structures. We, thus, reach a simple conclusion that the molecular weight affects only the transition temperatures. Returning to parts a and b of Figure 4, one can find that the isotropization temperature, T_2, increases with an initial increase of M_n and levels off at M_n more than 12 000 (approximately 30 repeat units). A similar trend has been reported.[3-8] On the other hand, the melting temperature of the crystal, T_1, decreases with an increase of M_n. As a result, the mesophase appears when M_n exceeds 4700 (corresponding to 13 repeating units) and its temperature region becomes expanded with an increase of M_n. The primary effect of increasing molecular weight, thus, is to stabilize the S_A phase. The increase of T_2 may be due to a preferable orientation of the side-chain mesogens resulting from sticking out perpendicularly to the main chain, but a reasonable explanation cannot be given for the decrease of T_1.

Figure 7. Optical fan-shaped texture observed for the smectic phase of poly(**1b**).

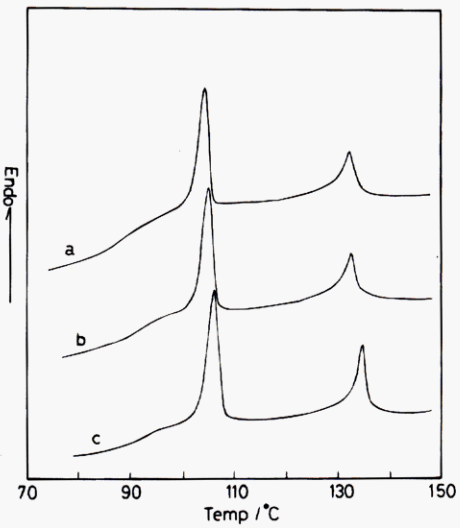

Figure 8. DSC heating thermograms of the block copolymers: (a) poly(**2a**); (b) poly(**2b**); (c) poly(**2c**).

Table 5. DSC Data of Polystyrene-*block*-poly(1)

	transition temp. °C (transition enthalpy, kcal/mol[a])			
	heating		cooling	
sample	T_1 (ΔH_1)	T_2 (ΔH_2)	T_1 (ΔH_1)	T_2 (ΔH_2)
poly(**2a**)	104.3 (0.77)	132.5 (0.45)	100.4 (0.77)	132.0 (0.45)
poly(**2b**)	105.4 (0.76)	132.8 (0.44)	101.0 (0.76)	132.1 (0.44)
poly(**2c**)	106.2 (0.83)	134.8 (0.49)	101.2 (0.81)	134.2 (0.46)

[a] Transition enthalpy as estimated per mole of MPPHM segment.

4. Thermotropic Phase Behavior and Structures of Block Copolymers. DSC thermograms of all the block copolymers are shown in Figure 8, and their thermodynamic data are listed in Table 5. From these data, the block copolymers are found to exhibit two transitions, similar to the homopolymers. Similarity is also observed in the phase sequence so that the crystal–S_A–isotropic phase transitions take place.

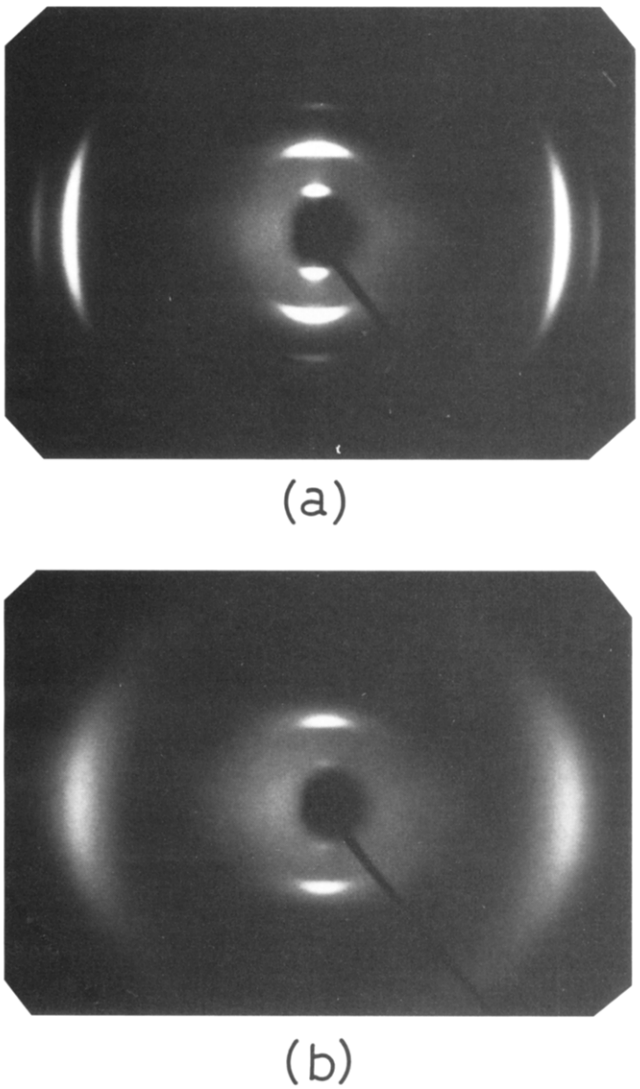

Figure 9. Oriented X-ray patterns of (a) the crystalline phase at 20 °C and (b) the smectic A phase at 110 °C in the fibrous block copolymer poly(**2a**). Here, the fiber specimen was prepared by drawing the isotropic melt, and its axis is placed in the vertical direction.

Parts a and b of Figure 9 show oriented X-ray patterns of crystal and S_A phases as observed for the fiber specimen of poly(**2a**) which was prepared by pulling up the isotropic melt. The deduced spacings for crystal and S_A phases are listed in Table 4 and found to correspond to those observed in the homopolymers. The fundamental microstructures of crystal and liquid crystal are thus essentially the same as those in the homopolymers. However, it must be noted here that two distinct structural aspects in the copolymers can be deduced from the oriented X-ray patterns of parts a and b of Figure 9. One is that the layer reflections appear on the equator. Hence, the layers in crystal and S_A phases are oriented perpendicular to the fiber axis. This orientation behavior is remarkably different from that observed in homopolymers in which the layers lie parallel to the fiber axis (refer to Figures 5 and 6). Another is that the layer reflections of the S_A phase are remarkably intense, and so the first layer reflection with a spacing of 26.4 Å as well as the intense second 13.2-Å reflection can be detected. These points are discussed in detail below.

The well-defined phase behavior as observed in the homopolymers shows that there is formed a segregation

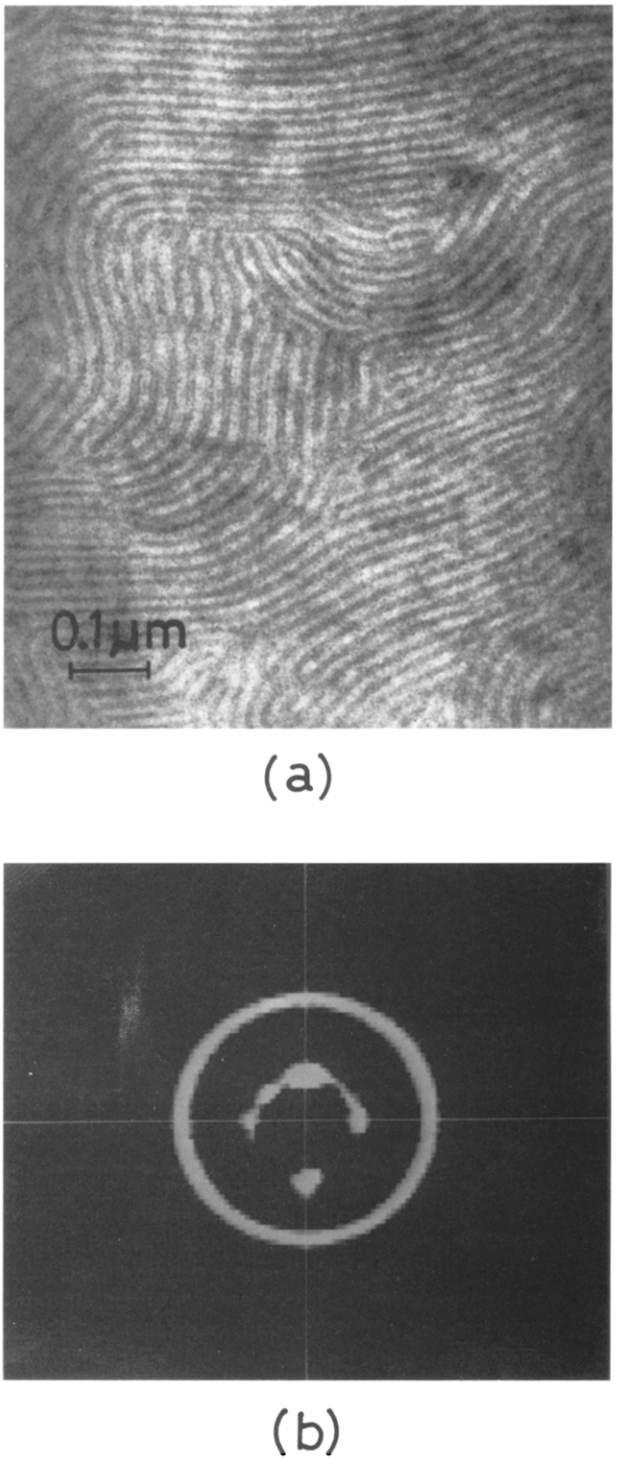

Figure 10. (a) TEM photograph and (b) small-angle X-ray pattern observed for the cast film of block copolymer poly(**2a**).

structure into amorphous polystyrene and liquid crystalline poly(**1**) microphases. In order to get information on the morphology, electron microphotographs were taken from the ultrathin sections cut out from the cast film and stained with ruthenium tetraoxide (RuO_4). Here, the cast film was prepared from a THF solution and annealed at 100 °C before observation. Figure 10a represents a typical electron microphotograph as observed in the poly(**2a**). It clearly demonstrates the microphase separation, with the liquid crystalline poly(**1**) microphases appearing dark because of staining with RuO_4. The phase boundary is very sharp, and the basic morphology is a lamellar type as expected from the

Table 6. Lamella Spacings (Å) of the Block Copolymers

sample	TEM	small-angle X-ray
poly(**2a**)	250	258
poly(**2b**)	250	252
poly(**2c**)	240	236

weight fractions of the block copolymers around 50%. Other specimens also show an identical lamellar type of morphology. The lamella spacings evaluated are listed in Table 6. The lamellar type of microphase separation was also observed from a small-angle X-ray diffraction method. Figure 10b shows a typical small-angle X-ray pattern which includes a sharp reflection. The reflection spacings corresponding to the lamella spacings are also collected in Table 6. One can find a quantitative correspondence between the lamella spacings due to both methods.

On comparison with the homopolymers, the block copolymers with microphase separation show several distinct features with respect to the transition behavior. At first, the smectic temperature region is fairly expanded. As can be found by comparing the copolymer with the homopolymer having a corresponding molecular weight, this expansion results mainly from a decrease in the melting temperature of the crystal since there is no significant difference in the isotropization temperature of the S_A phase. On this point, it is interesting to note that the crystal melting temperature is decreased as low as the glass transition temperature of polystyrene. We thus speculate that the crystal melting of a liquid crystalline segment may be triggered by the glass transition of a polystyrene segment. In fact, the DSC thermograms of the copolymers in Figure 8 suggest an overlapping of the glass transition and the crystal melting. The second point is that the transition enthalpies (ΔH) of both transitions are significantly smaller than those of homopolymers when they are evaluated per the poly(**1**) segment (compare Tables 3 and 5). The enthalpy change of crystal melting is roughly half of that in the homopolymer. Since the phase boundary is sharp on a local scale, this may be caused by an irregular structure at the interface; the poly(**1**) segment placed near to the phase boundary is in a disordered state, and only the segment in the interior of its microphase takes part in the crystallization. This effect may be weakened in the S_A phase since the ΔH of its isotropization is smaller by approximately 25% than that of the homopolymer.

Here, a question arises as to how the crystalline or S_A layer order correlates with the supermolecular lamellar order. In order to clarify this point, the oriented fiber specimen, which was prepared by pulling up the isotropic melt, was analyzed by electron microscopy and small-angle X-ray methods. The electron microphotograph of the fiber specimen is given in Figure 11a. One can find that the long-range lamellae are oriented preferentially in the direction of the fiber axis. The same result can be deduced from the small-angle X-ray diffraction pattern that is shown in Figure 11b. These results are interestingly compared with the previous result obtained from the wide-angle X-ray diffraction pattern of parts a and b of Figure 9, in which the crystal and liquid crystalline layers are formed perpendicularly to the fiber axis. From this comparison, it is obvious that the crystal and smectic layers in block copolymers are oriented preferentially normal to the supermolecular lamellae. The situation is schematically illustrated in Figure 12.

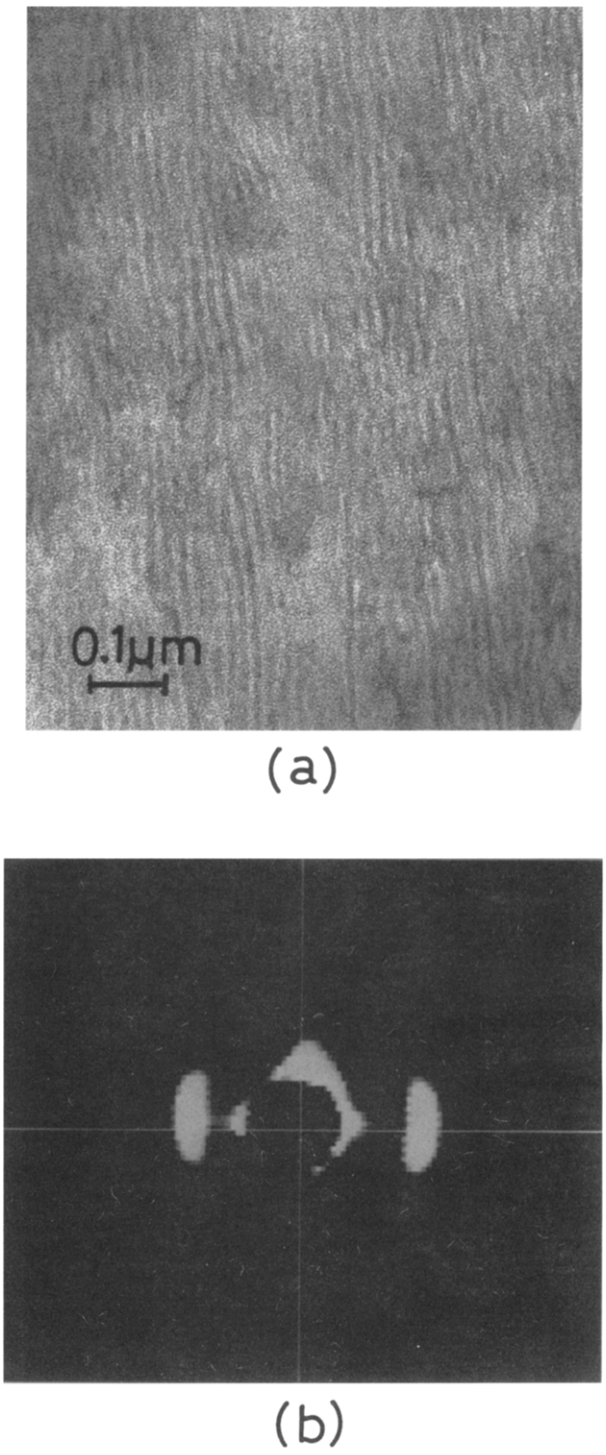

Figure 11. (a) TEM photograph and (b) small-angle X-ray pattern observed for the oriented fiber of block copolymer poly(**2a**). Here, the oriented fiber was prepared by drawing the isotropic melt, and its axis is placed in the vertical direction.

Why does a perfect orientation correlation arise between the macroscopic lamellar order and the microscopic layer order? At this time, we suppose that this correlation has been promoted by the main-chain backbone of the poly(**1**) block. In the microphase separation systems, it is likely that the main-chain backbone tends to orient perpendicular to the interface of two microphases.[27] Further, the previous X-ray data show that in the crystalline and smectic phases the main chains tend to have an oblate conformation so as to be placed between the mesogenic layers.[25,26] Such a restricted

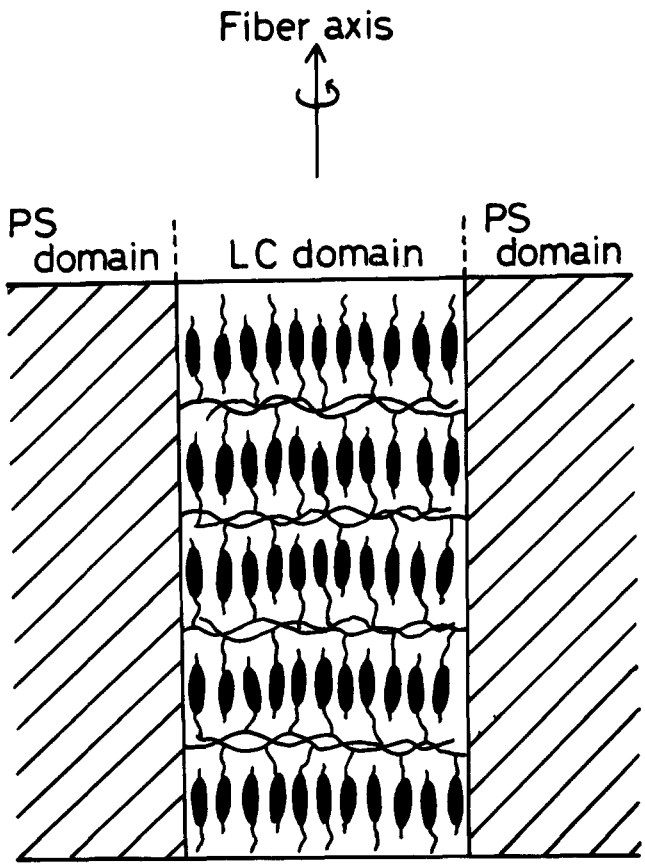

Figure 12. Schematic illustration of the oriented layer structure in the fibrous block copolymer as elucidated from the data in Figure 11.

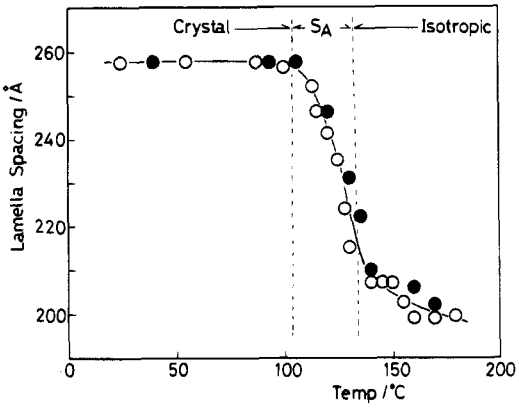

Figure 13. Temperature dependence of the lamella spacing in the microphase segregation structure as observed in the block copolymer poly(**2a**); (○) heating data and (●) cooling data..

orientation of main chains may force the side-chain mesogenic groups to form the layers perpendicularly to the interface and also with the higher layer order parameter. Similar orientation correlation has been reported by Adams and Gronski[12,13] and explained by the same basis.

Finally we refer to the temperature dependence of lamella spacing. Its typical example, as observed for poly(**2a**) by the small-angle X-ray method, is shown in Figure 13. It demonstrates that the lamellar type of microphase is invariably observed through the whole temperature region from crystal to isotropic melt and the lamella spacing decreases remarkably from 250 Å of the crystalline phase to 200 Å of the isotropic phase after a steady decrease in the S_A temperature region. The overall change in the lamella spacing is as large as one-fifth of the lamella spacing and was found to be completely reversible on heating and cooling cycles. Considering that the association of the side-chain mesogens into a layer is not essentially altered on the transition from crystal to S_A and also through the S_A temperature region, such a reversible change in the lamella spacing is obviously caused by the conformational change of the main-chain backbone, possibly from the more extended form in the crystal to the random-coil form in the isotropic phase. The detailed analysis is now proceeding on this interesting phenomenon and will be reported elsewhere.

Conclusion

Living anionic polymerization was successfully performed to prepare a series of side-chain liquid crystalline poly(**1**) with a well-controlled structure. Polymerization was attempted at an elevated temperature of −40 °C since precipitation occurs during the polymerization at an usually applied temperature of −78 °C. Irrespective of this unusual condition for the living anionic polymerization, the polymers were obtained with the unimodal distribution of more or less than 1.1 when the molecular weights are less than 12 000. All the polymers except for the lowest molecular weight polymer with repeat units of 9 exhibit the crystal, S_A, and isotropic phases, showing that the molecular weight does not significantly affect the phase sequence and phase structures. Only an effect can be observed on the transition temperatures. The isotropization temperatures increase with the molecular weight and level off when the number of repeat units exceeds 30, while the melting temperature of the crystal decreased gradually. As a result, the smectic A phase is stabilized with an increase of the molecular weight.

Block copolymers with amorphous polystyrene were also prepared with a well-defined structure. These copolymers were found to show a lamellar type of microphase separation with the sharp phase boundary and the side-chain liquid crystalline block in its microphase turned out to exhibit transitions similar to those of the homopolymers. The temperature region of the smectic phase is more expanded than that of the homopolymer, which was caused mainly by a decrease of the crystal melting temperature. In this segregation system, two distinct structural characteristics were elucidated. One is that the side-chain mesogenic groups are organized to form the crystalline and smectic A layers with their long axes oriented perpendicular to the interphase of the lamellar domian. Another is that the lamella spacing is decreased to a great extent through transitions from the crystal to istropic phase after a steady decrease during the smectic A temperature region. These phenomena may be understood by considering the confinement effect exerted by the crystal and smectic fields on the main-chain backbone.

References and Notes

(1) McArdle, C. B. *Side Chain Liquid Crystal Polymers*; Chapman and Hall: New York, 1989.
(2) Collyer, A. A. *Liquid Crystal Polymers*; Elsevier Applied Science: London and New York, 1992.
(3) Percec, V.; Tomazos, D.; Pugh, C. *Macromolecules* **1989**, *22*, 3259.
(4) Percec, V.; Lee, M. *Macromolecules* **1991**, *24*, 1017; **1991**, *24*, 2780.
(5) Sagane, Z.; Lenz, R. W. *Macromolecules* **1989**, *22*, 3763.
(6) Komiya, Z.; Pogh, C.; Schrock, R. R. *Macromolecules* **1992**, *25*, 3609; **1992**, *25*, 6586.

(7) Papon, E.; Deffieux, A.; Hardouin, F.; Achard, M. F. *Liq. Cryst.* **1992**, *11*, 803.
(8) Bohnert, R.; Finkelmann, H.; Lutz, P. *Makromol. Chem., Rapid Commun.* **1993**, *14*, 139.
(9) Finkelmann, H.; Happ, M.; Portugal, M.; Ringsdorf, H. *Makromol. Chem.* **1978**, *179*, 2541.
(10) Hahn, B.; Wendorf, J. H.; Portugal, M.; Ringsdorf, H. *Colloid Polym. Sci.* **1981**, *259*, 875.
(11) Nakano, T.; Hasegawa, T.; Okamoto, Y. *Macromolecules* **1993**, *26*, 5494.
(12) Adams, J.; Gronski, W. *Makromol. Chem., Rapid Commun.* **1989**, *10*, 553.
(13) Adams, J.; Gronski, W. *In Liquid-Crystalline Polymers*; Weiss, R. A., and Ober, C. R., Eds.; ACS Symposium Series 435; Amercial Chemical Society: Washington, DC, 1990; p 174.
(14) Komiya, Z.; Schrock, R. R. *Macromolecules* **1993**, *26*, 1387.
(15) Bohnert, R.; Finkelmann, H. *Makromol. Chem. Phys.* **1994**, *195*, 689.
(16) Fayt, R.; Forte, R.; Jacobs, C.; Jérôme, R.; Ouhadi, T.; Teyssié, Ph.; Varshney, S. K. *Macromolecules* **1987**, *20*, 1442.
(17) Varshney, S. K.; Hautekeer, J. P.; Fayt, R.; Jérôme, R.; Teyssié, Ph. *Macromolecules* **1990**, *23*, 2618.
(18) Ozaki, H.; Hirao, A.; Nakahama, S. *Macromolecules* **1992**, *25*, 1391.
(19) Mori, H.; Hirao, A.; Nakahama, S. *Macromolecules* **1994**, *27*, 35.
(20) Hahn et al.[10] reported the monoclinic lattice for the crystal of the same polymer. However, this type of lattice cannot explain the overall reflections observed here.
(21) Trotter, J. *Acta Crystallogr.* **1961**, *14*, 1135.
(22) Watanabe, J.; Tominaga, T. *Macromolecules* **1993**, *26*, 4032.
(23) Gudkov, V. A. *Sov. Phys. Crystallogr.* **1984**, *29*, 316.
(24) Keller, P.; Carvalho, B.; Cotton, J. P.; Lambert, M.; Moussa, F.; Pepy, G. *J. Phys. Lett.* **1985**, *46*, L-1065.
(25) Davidson, P.; Strzelecki, L. *Liq. Cryst.* **1988**, *3*, 1583.
(26) Davidson, P.; Levelut, A. M.; Achard, M. F. *Liq. Cryst.* **1989**, *4*, 561.
(27) Aggarwal, S. *Block Copolymers*; Plenum Press: New York, 1970.

MA941004P